

10

Circuits and components

Circuit basics were covered in block-diagram form in Chapter 4. This chapter presents more design details, including schematics and component specifications. Capacitor dielectric properties are discussed in detail.

10.1 CAPACITOR DIELECTRICS

Considerable research on capacitor dielectrics was done at the Laboratory for Insulation Research at MIT in the 1950s and 1960s, and it is reported in a number of publications. In 1954, von Hippel discusses macroscopic and molecular properties of dielectrics, analyzes several dielectric applications, and presents an extensive list of dielectric parameters for many materials which has been condensed to Appendix 2. This laboratory also has published research into the dielectric properties of biological materials, materials at high temperatures, and measurement techniques.

The *IEEE Transactions on Dielectrics and Electrical Insulation* reports on recent developments in dielectric research.

10.1.1 Classical dielectric models

A lossy capacitor is classically modeled as a lossless capacitor with either a series or shunt resistor representing the loss term (Figure 10.1).

The series parasitic inductance L and the series resistance R_s can usually be ignored for our low current applications, or R_s can be converted to R_p for a particular frequency using

$$R_p = \frac{X_c^2}{R_s} = \frac{1}{(2\pi fC)^2 R_s} \quad 10.1$$

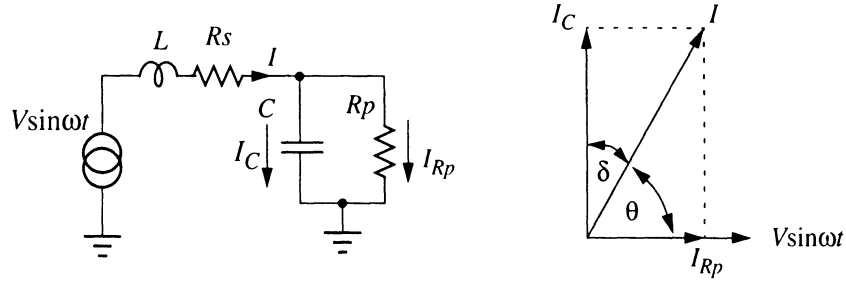


Figure 10.1 Lossy capacitor

The phasor diagram above (with R_s and L ignored) shows the relationship of the applied AC voltage to the in-phase current through the resistance and the 90° current through the capacitor. The capacitor *dissipation factor* D , also called *loss tangent*, $\tan \delta$, is the ratio of capacitive reactance X_C to resistance defined as

$$D = \frac{1}{Q} = \tan \delta = \frac{R_s}{X_C} = \frac{R_p}{R_p} = \frac{1}{\omega R_p C} \quad 10.2$$

As frequency increases, I_C increases while I_{Rp} remains constant, so D decreases with increasing frequency if R_p is constant.

A similar dimensionless figure of merit is the power factor, defined as

$$PF = \frac{\text{power dissipation}}{\text{volts} \cdot \text{amperes}} \quad 10.3$$

For $Q > 10$, PF is close to D .

The value of the equivalent lossless capacitor C is usually relatively independent of frequency over a wide range, but the behavior of the loss component R_p is not as simple. Various mechanisms contribute to loss, including actual conductivity due to migrating charge carriers and friction associated with the reorientation of polar molecules. Most commonly used dielectrics have a loss tangent which is relatively independent of frequency, implying that R_p decreases directly with an increase in ω . Figure 10.2, with data taken at various temperatures [von Hippel, 1954], shows that with the exception of Steatite ceramic (uncommonly used for capacitor dielectrics), loss tangent is remarkably constant with frequency. The loss tangent of the classic RC model with constant R_p is also plotted. The loss tangent remains relatively and remarkably constant through 16 frequency decades, 10^{-4} Hz– 10^{12} Hz, for common capacitor dielectrics.

10.1.2 Modified dielectric model

The classic capacitor model (Section 10.2.1) is valid for a single frequency, but it does not account for the constant loss tangent with frequency. It also does not model two additional capacitor characteristics which can be observed empirically, dielectric absorption and insulation resistance change (or, equivalently, leakage current increase) vs. time.

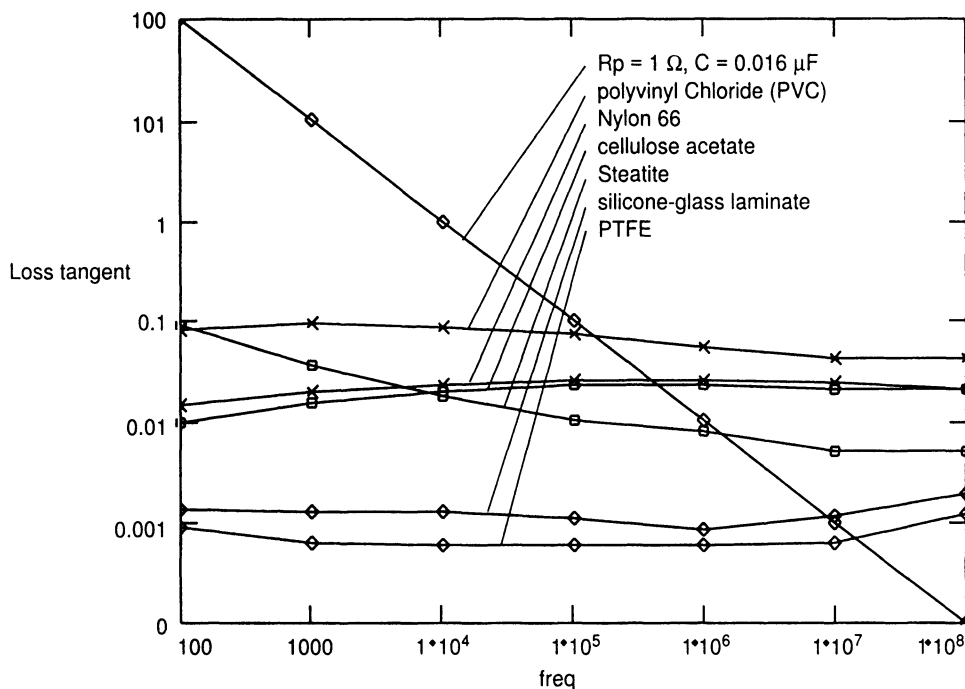


Figure 10.2 Loss tangent of various materials vs. frequency [von Hippel, 1954]

Dielectric absorption

Dielectric absorption is the excess charge absorbed, ignoring the normal charge expected from the equation $Q = CV$, by a capacitor polarized with a DC voltage. It is measured by charging a capacitor for 1 h at rated DC voltage and discharging through a $5\ \Omega$ resistor for 10 s. When the resistor is disconnected and the capacitor is open circuited, a percentage of the impressed voltage returns. The magnitude of this voltage is measured 15 min later. Some typical values of dielectric absorption are shown in Table 10.1.

Table 10.1 Dielectric absorption [Excerpted from (Westerlund). Copyright ©1994 by the Institute of Electrical and Electronics Engineers.]

	Dielectric absorption	$\tan \delta$	RC , seconds	n
Metalized paper	10%	0.028	3100	0.9821
PET (polyethylene-terephthalate)	1%	0.0025	38,000	0.9984
Polypropylene	0.003%	0.000075	1,250,000	0.999952

Table 10.1 also lists the self-discharge time constant (the product of the insulation resistance and the capacitance, RC) and a constant n which is related to the quality of the dielectric, as shown below.

Empirical model

Westerlund [1994] presents an empirical model of capacitor behavior which models the observed variation of R with frequency, and also models the decrease in capacitor leakage current vs. time. This model replaces C in Figure 10.1 with C_0 , with C_0 very nearly equal to C for good dielectrics, and replaces Rp with

$$R_n \approx \frac{h_1(1-n)}{\cos\left(\frac{\pi n}{2}\right)\omega^n} \quad 10.4$$

where h_1 is a constant related to capacitance. Westerlund's model closely tracks the observed charge absorption and insulation resistance change of common capacitor dielectrics, and it is considerably more accurate at predicting effects like the variation of leakage current vs. time and charge absorption than the standard RC capacitor model.

Insulation resistance vs. time

A constant DC voltage V applied to a capacitor C at $t = 0$ will produce a leakage current, in excess of normal capacitor charging current, of

$$i(t) \approx \frac{VC}{\left(\frac{1}{1-n}\right)t^n} \quad 10.5$$

For a very good capacitor dielectric such as polypropylene, n (from Table 10.1) is close to 1 and i will be near zero. This equation implies that the insulation resistance R of a capacitor varies with time as t^n after applying a DC voltage.

10.1.3 Other dielectrics

Figure 10.2 shows that for a selection of miscellaneous plastics and ceramics the loss tangent is relatively constant vs. frequency. In most of these materials, the dielectric constant varies by less than 2:1. In contrast with the stable loss tangent of capacitor dielectric materials, the loss tangents of the miscellaneous materials shown in Figure 10.3 vary by factors of 100. Especially active is water, which is also responsible for the large change in loss tangent of materials like leather and paper for different relative humidities.

The relative dielectric constant of water is very high at about 80, and shows large changes with temperature; in Figure 10.4, water is shown with an expanded frequency range (note the nonlinear x axis). Measurement of water below 100 kHz is difficult because the angle of the loss tangent is nearly 90° . At 100 kHz, the loss tangent of 4 means that the impedance has an angle of 76° ; the resistive component has a much lower impedance than the reactive component.

Dielectric measurement (Figure 10.5) has been suggested for the measurement of biological material properties [von Hippel, Oct. 1954], such as changes in cell permeability and cell content. Generally the loss tangent is a more sensitive indicator than dielectric constant. Aviation gasoline tested in Appendix 2 shows a change in loss tangent at 10 kHz from 0.0001 to 0.0004 as octane decreases from 100 to 91, while the dielectric constant change is from 1.94 to 1.95.

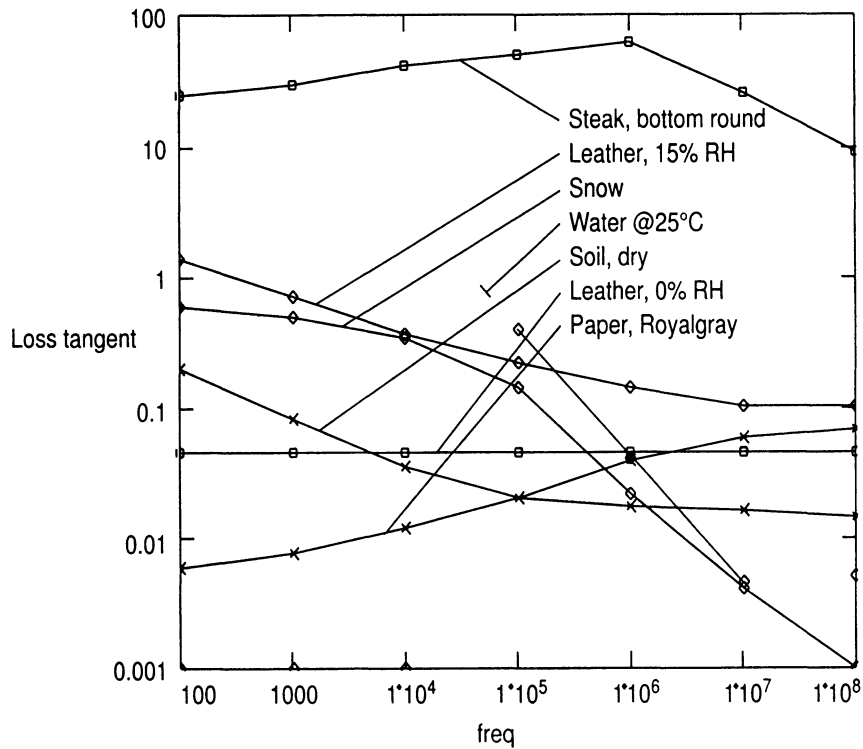


Figure 10.3 Loss tangent vs. frequency [von Hippel, 1954]

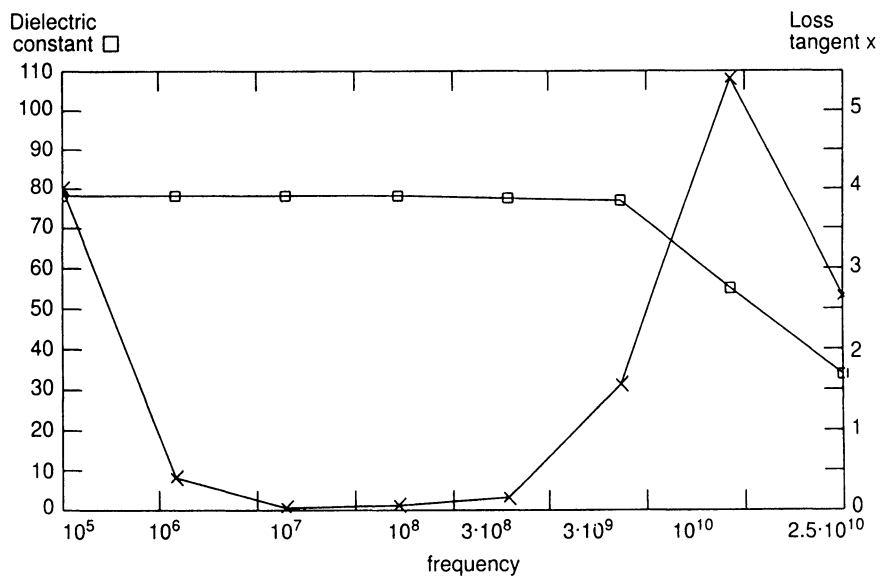


Figure 10.4 Dielectric constant and loss tangent of water vs. frequency at 25°C

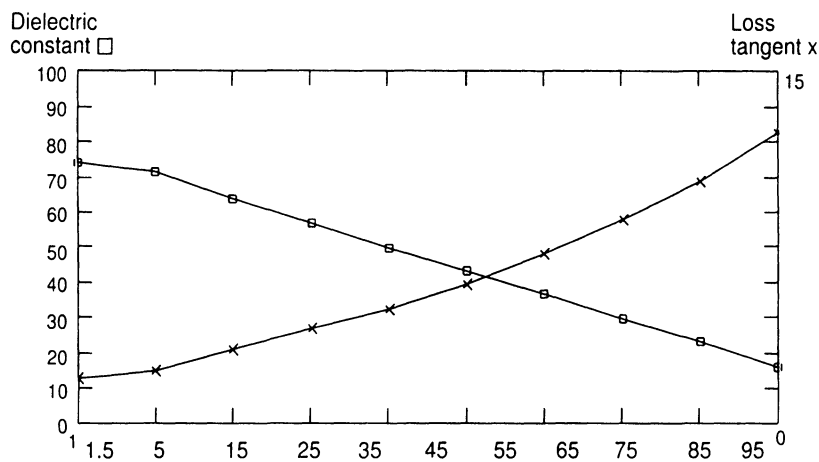


Figure 10.5 Dielectric constant and loss tangent of water vs. temperature at 1 MHz [von Hippel, 1954]

Another behavior of dielectric molecules is shown in this chart of Neoprene rubber (Figure 10.6). Polar molecules such as water and Neoprene often produce a temperature-sensitive peak in loss tangent, caused by a molecular resonance effect. As temperature is increased, the peak frequency will increase. The change of loss tangent may also be accompanied by a change in dielectric constant.

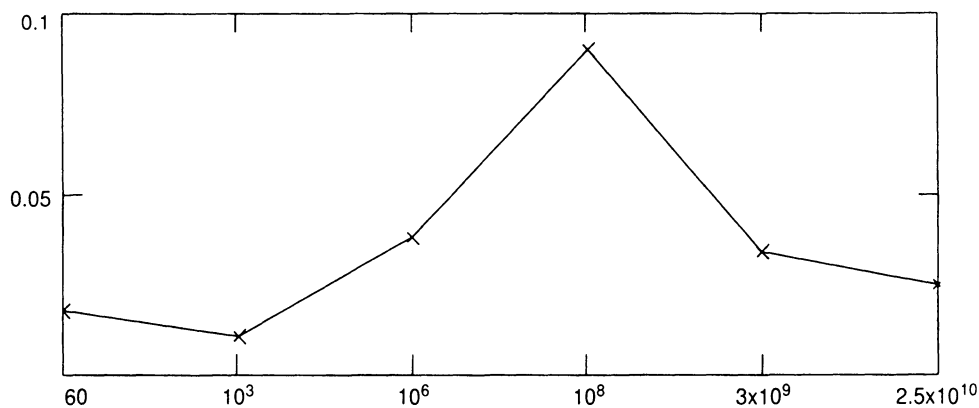


Figure 10.6 Neoprene loss tangent vs. frequency

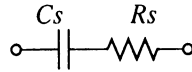
10.2 CAPACITOR MEASUREMENT

10.2.1 Capacitor models

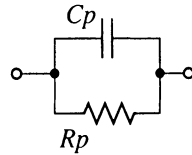
For low frequencies, two models are possible: the series model and the parallel model. Either model accurately represents the capacitance and the loss tangent of a capacitor at any single frequency. The parallel model is preferred, however, as the leakage current at DC is represented, and also if the dielectric is changed, the calculation of the new dielec-

tric constant is simple, as the ratio of dielectric constants changes directly with the change in C_p . At higher frequencies three-terminal and four-terminal models including R , L , and C are used [East, 1964] to model the more complicated behavior of polar molecules.

Series



Parallel



10.2.2 Bridges

The Schering bridge (Figure 10.7) is used for measuring capacitor and dielectric parameters [Reference Data for Engineers, p. 12-5].

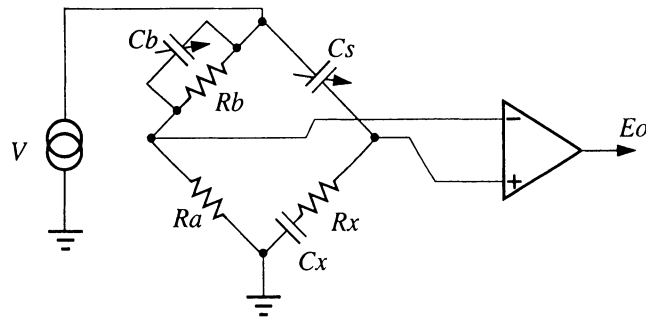


Figure 10.7 Schering bridge

The capacitor under test is $C_x R_x$, and the amplifier is usually an instrumentation amplifier rather than an operational amplifier so the gain is stable and well defined. The following calculation is used when the bridge is adjusted to null.

$$C_x = C_s \cdot \frac{R_b}{R_a}$$

$$\frac{1}{Q_x} = \omega C_x R_x = \omega C_b R_b$$

If a parallel model for the capacitor is needed, a modified Schering bridge is used, an example of which is shown in Figure 10.8.

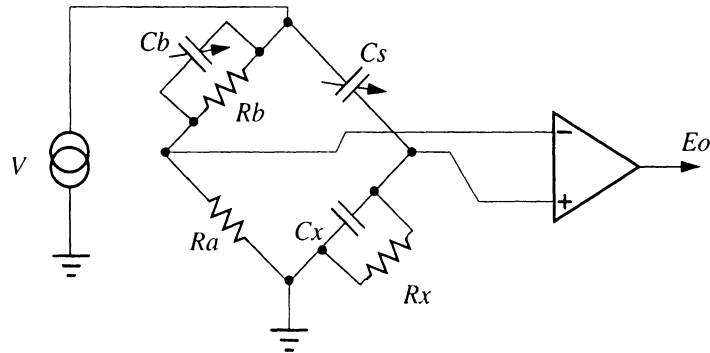


Figure 10.8 Modified Schering bridge

A carefully constructed Schering bridge for dielectric property measurements [Charles, 1966] has a loss angle sensitivity of 10^{-6} rad at frequencies of $1\text{--}10^5$ Hz.

10.3 PICKUP AMPLIFIERS

For capacitive sense systems with moderate resolution requirements, the pickup amplifier can be replaced by a simple comparator, or circuits such as an oscillator or a one-shot can be used. For circuits needing more accuracy a synchronous demodulator is needed, and the pickup amplifier needs higher precision and should be carefully matched to the application.

For good performance, the amplifier should have a high impedance input with low voltage noise and current noise at the excitation frequency. The circuit configuration may be a high-Z type, where the amplifier is used as a follower and has very high input impedance, or a low-Z type, where the amplifier's inverting input terminal is used as an input and heavy feedback results in low input impedance. A third option includes the sensor in the feedback loop and has some characteristics of each. These circuits are summarized in Chapter 3 and more fully discussed here.

10.3.1 High-Z amplifier

The guarded high-Z amplifier (Figure 10.9) is similar to circuits shown in Chapter 4, with an operational amplifier driving a guard to reject stray capacitance and to provide a shield against ambient electrostatic fields. Although this circuit is adequate for sensors with high sensor capacitance, above roughly 50 pF, it will be found unacceptable for smaller sensor capacitance because of amplifier parasitic input capacitance. In the figure above an additional bootstrap connection through C_v is brought to the V_{ee} terminal of the amplifier. This connection nulls out the amplifier's internal capacitance from V_{ee} to the input terminal and can improve the amplifier common-mode input capacitance from 5–10 pF to a fraction of a pF. Some electrometer-type amplifiers such as the AD549 and OPA129 (see Table 10.2) have 1 pF of common mode input capacitance and may not need V_{ee} bootstrapping.

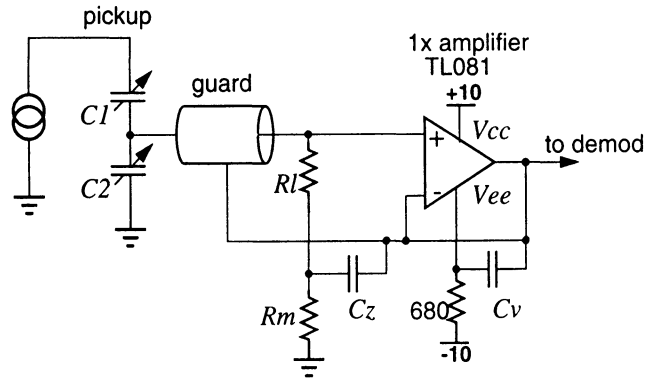


Figure 10.9 Guarded high-Z amplifier

Input resistance

The input resistance, R_I in Figure 10.9, is used to provide a path for amplifier input bias current and to set the input voltage to near zero, but it tends to shunt the signal and cause a spacing-dependent loss of output voltage with low-capacitance sensors. Figure 10.9 shows a way to bootstrap input resistance to higher values. The load resistor R_I is bootstrapped through C_z to the amplifier's output. With C_z large, this increases the effective value of R_I by a factor equal to the amplifier open-loop gain.

With a signal capacitance of 1 pF and a clock frequency of 20 kHz, the input time constant without C_z is $R_I \times 1$ pF. As the time constant should be about 1/10 of the clock period for good waveshape, an input resistance of 500 M Ω is needed which is not only difficult to purchase, but can mandate a strenuous design effort to minimize stray currents. Strays caused by board leakage and op amp input bias current can affect gain and offset. With bootstrapping, a more convenient resistor value such as 10 M Ω can be used, and no problems will be encountered with stray current due to op amp input current or printed-circuit-board surface conductivity.

The value of C_z must be carefully chosen, as the bootstrap circuit may oscillate with some values. A SPICE simulation to check stability is recommended (Figure 10.10).

```
.define C1 10u
.define R1 22meg
.define R2 1k
```

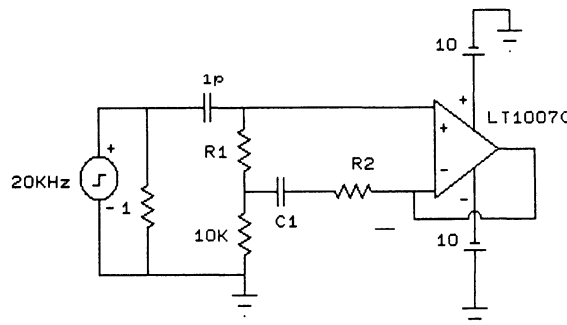


Figure 10.10 SPICE circuit of bootstrapped high impedance amplifier

These results were calculated (Figure 10.11). With low values of R_2 , considerable peaking is produced at 100 Hz which will usually cause the circuit to misbehave. As R_2 is increased, this peaking disappears, but the bootstrap effect decreases; with $R_2 = 100$, the gain peaking is minimal, but the bootstrap amplification of input impedance is reduced to $10\times$, or 220 M Ω . Bootstrapping can be useful for moderate increases of input resistance, but for high input impedance without peaking, start with the largest possible value of R_1 and use other measures as described in Chapter 13 to interrupt leakage current.

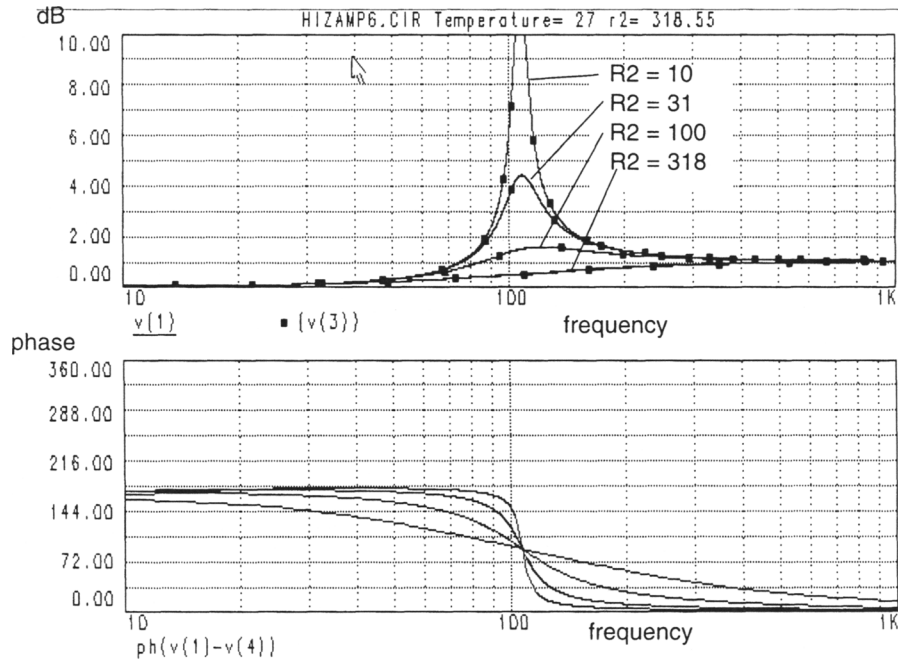


Figure 10.11 SPICE analysis of bootstrapped high-Z circuit

Stray capacitance

Several parasitic capacitances are found in an operational amplifier, including:

1. Capacitance between + and - inputs, which can often be found on the amplifier's spec sheet and is typically a few pF
2. Capacitance between + input and V^- input
3. Capacitance between + input and V^+ input

Capacitances 2 and 3 are not listed on the typical spec sheet, and they are not included in SPICE models. Some recent amplifiers do specify these capacitances; Texas Instruments' TLE2071 lists common mode input capacitance as 11 pF and differential-mode input capacitance as 2.5 pF. These strays can be handled in different ways:

- Capacitance 1 is not a concern as the negative input tracks the positive input and no current can flow in this capacitance, except if it is much larger than the sensor capacitance the output noise and rise time increase
- Capacitance 2 can be bootstrapped out by use of C_v as shown above
- Capacitance 3 cannot be bootstrapped in the typical integrated amplifier, as the $V+$ input is usually used as a gain stage reference voltage, and attempting to bootstrap it ruins the amplifier's gain

Parasitic capacitance simulation

Differential- and common-mode parasitic op amp capacitances are not included in SPICE operational amplifier models. If the typical 2 pF parasitic capacitances are added externally, the SPICE model of a high-Z amplifier becomes as shown in Figure 10.12.

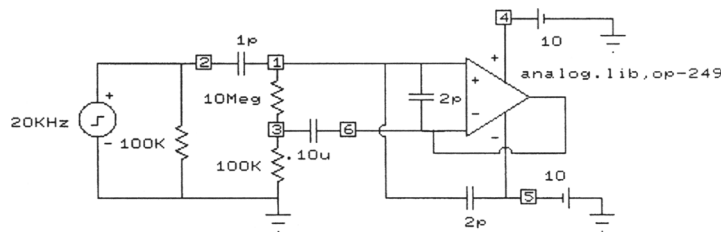


Figure 10.12 High-Z amplifier with parasitic capacitance

This amplifier shown is driven with a small, 1 pF sensor capacitance. With the attenuation of the parasitic capacitance, the output will have low amplitude and it will be very sensitive to the exact value of sensor capacitance. This may contribute an unwanted spacing sensitivity. The response with a 5 V square wave excitation is shown in Figure 10.13. The 2 pF capacitance to V_{ee} is attenuating the signal by 3 \times .

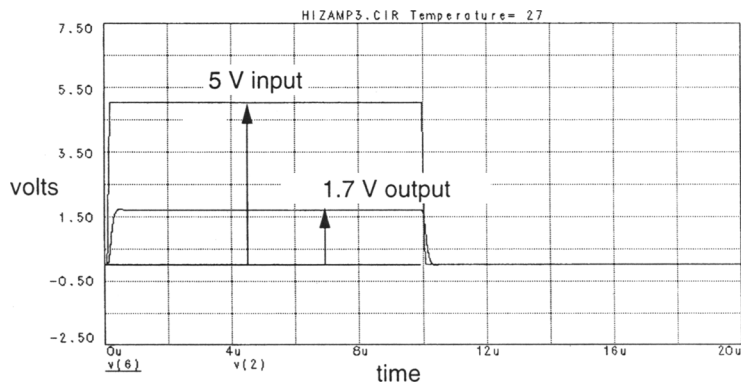


Figure 10.13 High-Z amplifier transient response

Adding a capacitor to bootstrap the V_{ee} rail of the op amp as Figure 10.9 produces the SPICE circuit shown in Figure 10.14, featuring a much more accurate AC gain.

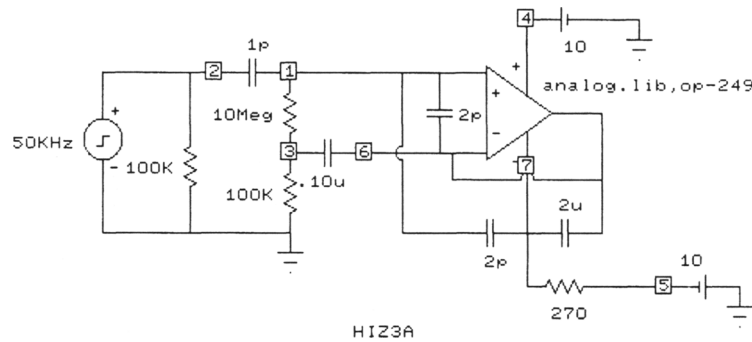


Figure 10.14 High-Z amplifier, bootstrapped *Vee*

The AC response can be tested for peaking. The component values shown in Figures 10.15 and 10.16 produce a bridged-T notch response which will not impair circuit operation.

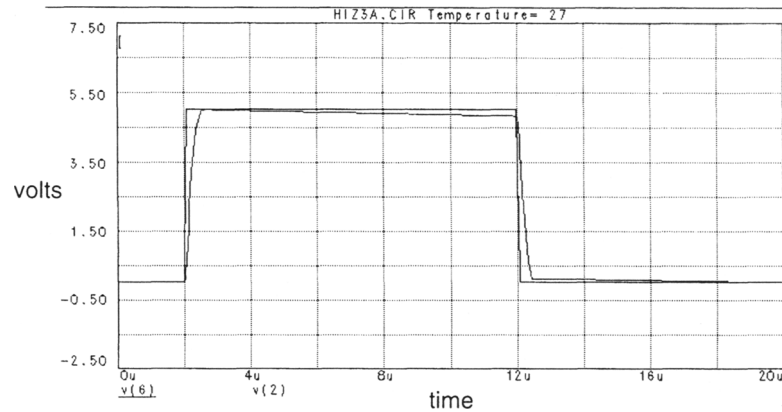


Figure 10.15 High-Z amplifier, bootstrapped *Vee*, transient response

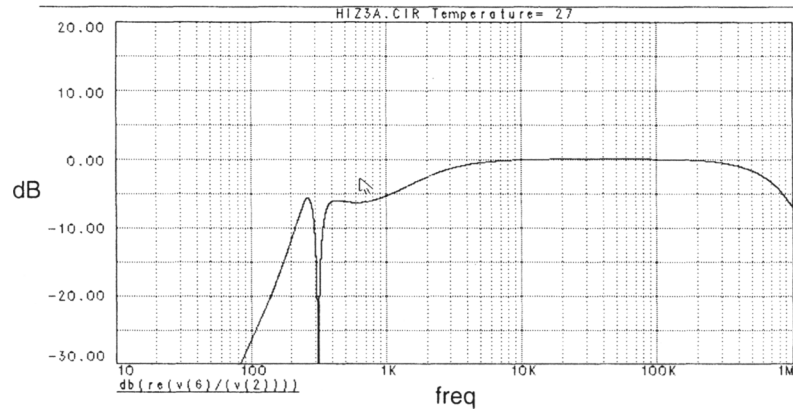


Figure 10.16 High-Z amplifier, bootstrapped *Vee*, AC response

Stabilizing the bootstrap connection

There is a hazard when bootstrapping V_- . The positive feedback will make many amplifiers unstable (although not the TL081 shown), and cause oscillation at a frequency near the amplifier's f_T . This can be fixed by adding a lowpass filter to the bootstrap with a break frequency between the amplifier f_T and the frequency of the capacitive sensor drive (Figure 10.17).

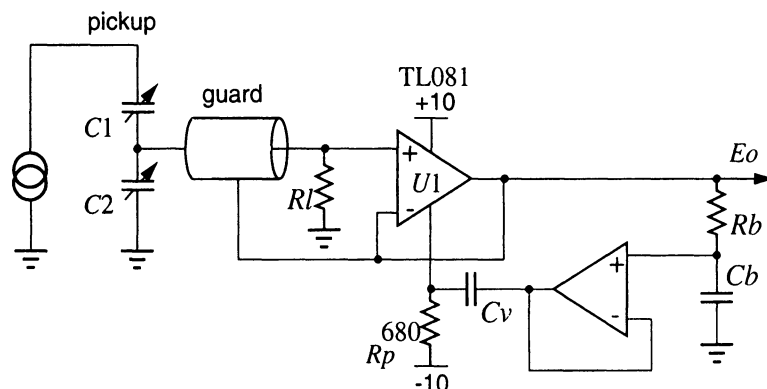


Figure 10.17 Stabilized bootstrap connection

The 3 dB frequency of the lowpass filter R_b, C_b should be about $1/4 - 1/10$ of the amplifier's f_T . R_p is chosen to drop 2 or 3 V at the chosen amplifier's supply current, and C_v is chosen for an $R_v C_v$ time constant considerably longer than the period of the clock. A single op amp should be used for U_1 rather than a dual or quad to keep total supply current low. This circuit works well with sensor capacitance greater than about 5 pF. Rise and fall times are about 5 μ s, so signal clock frequency should be 10–50 kHz.

10.3.2 Rise time effects

Rise time change with spacing

As plate spacing increases and the sensor capacitance drops, the output rise time decreases proportionally. This is illustrated by the equivalent circuit (Figure 10.18).

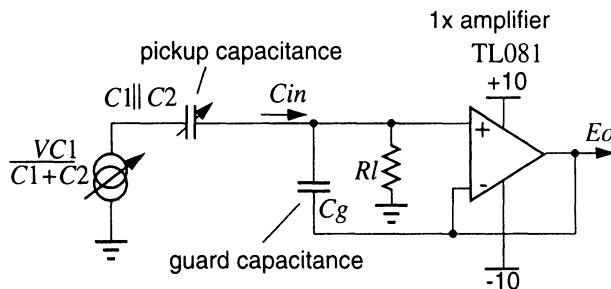


Figure 10.18 Rise time analysis

If the closed-loop amplifier gain is 1, C_g is fully bootstrapped out and C_{in} is zero or perhaps 1–2 pF of parasitic capacitance. If the closed-loop amplifier gain drops to K , how-

ever, the input capacitance increases to $C_g \times (1 - K)$. If, for example, the pickup plate is formed as an etch pattern on the top of a 0.062 in glass-epoxy printed circuit board (dielectric constant = 6) and the guard is formed with a similar etch pattern on the bottom, and assuming the signal electrodes were air-spaced at 0.062 in, C_g would be six times the pickup capacitance, $C_1 \parallel C_2$. If a signal frequency of 25 kHz and an amplifier with 2.5 MHz f_T and 6 dB/octave compensation is used, the amplifier gain at 25 kHz would be 2.5 MHz/25 kHz or 100 and closed loop gain drops to 0.99. The signal fundamental would be attenuated by 1%. Harmonics would be attenuated at a 6 dB per octave rate, so a square waveform will become somewhat rounded. As the spacing is further increased, the fundamental at 25 kHz will be more severely attenuated. To minimize this problem, maximize pickup capacitance, choose an op amp with high f_T and minimize C_g .

Slew rate limit

Another effect is the amplifier slew rate limit tabulated in Table 10.2. The high frequency reduction shown is a gain change only, but slew rate effects are nonlinear, produce a temperature-dependent kink in the transfer function, and should be avoided by selecting a high slew rate amplifier, using sine wave or trapezoidal excitation, preceding the amplifier with a lowpass or bandpass filter, or using a demodulator circuit that samples the amplifier output after the voltage has stabilized.

10.3.3 Discrete amplifiers

For applications with small sensor capacitance needing a high frequency clock, say over 100 kHz, the operational amplifier can be replaced with a discrete JFET or MOSFET amplifier, with suitable bootstrapping to reduce stray capacitance. Discrete amplifiers have good performance at a sacrifice of DC output precision, but DC offset is not usually a significant problem. A compound follower circuit with a small-geometry MOSFET (SD213) has a broadband high input impedance (Figure 10.19),

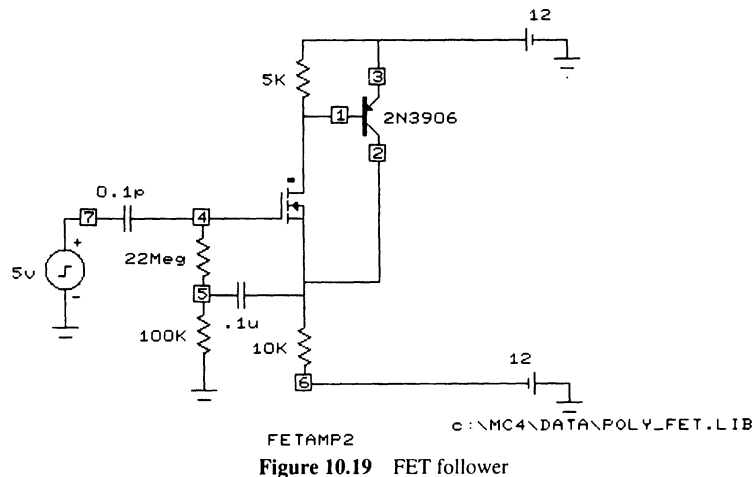


Figure 10.19 FET follower

with the FET gate-to-source capacitance, C_{GS} , bootstrapped out by the follower connection. The remaining capacitance from gate to drain is smaller, about 0.2 pF, but will cause

serious attenuation with the small 0.1 pF sensor capacitance illustrated. The response to a 5 V square wave shows that the input capacitance is about 0.5 pF (Figure 10.20).

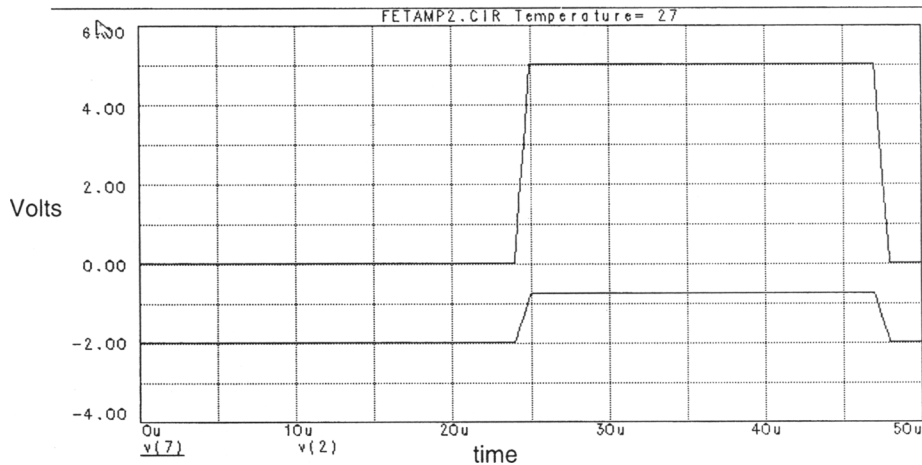


Figure 10.20 FET follower, transient response

A plot of AC gain vs. frequency shows the expected low frequency peaking caused by the input bootstrap (Figure 10.21). Although the V_{cc} rail cannot usually be bootstrapped with an integrated amplifier, the compound follower circuit can be bootstrapped to remove the effects of the FET gate-to-drain capacitance as shown in Figure 10.22, where $R1$ - $C1$ help to minimize the amplitude of a 50 MHz high frequency peak. This circuit exhibits an input capacitance much smaller than the 0.1 pF sensor capacitance. The transient response shows about 95% amplitude which translates to a capacitance of 0.005 pF at the input (Figure 10.23).

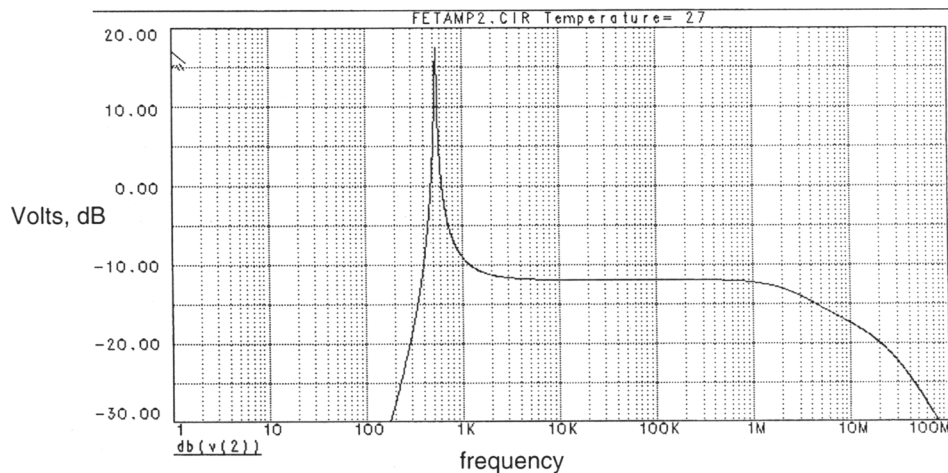


Figure 10.21 FET follower AC gain

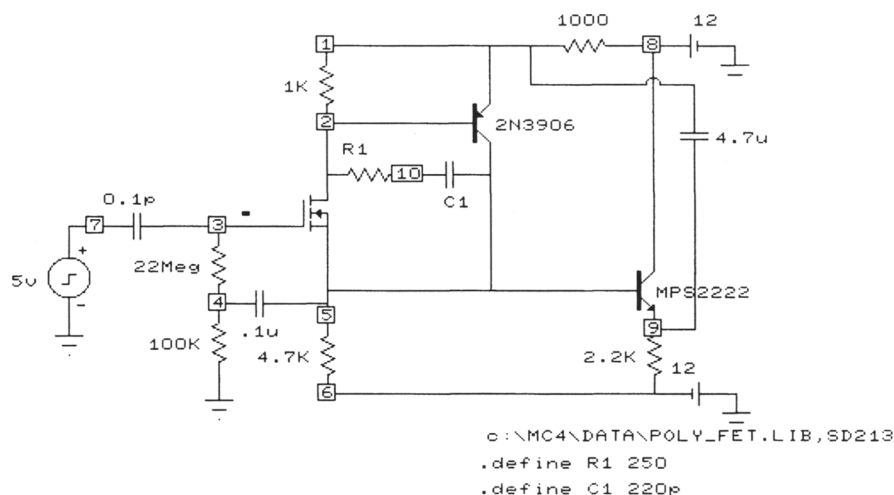
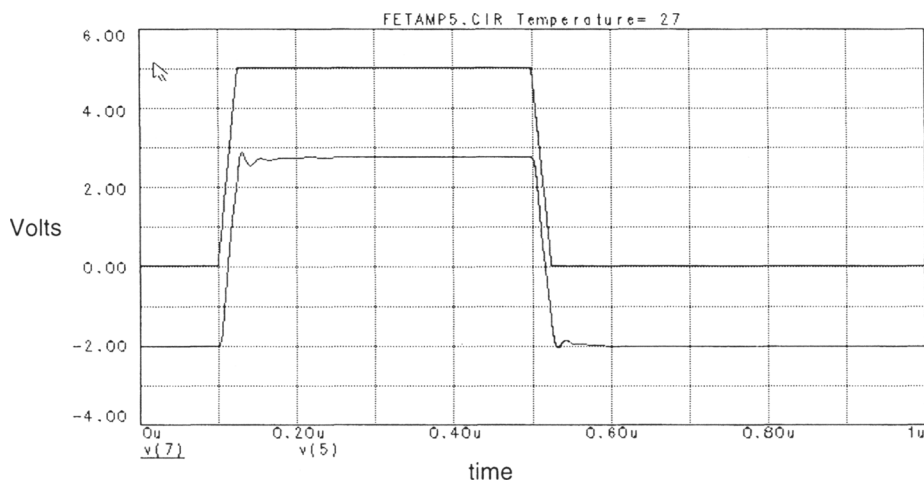


Figure 10.22 Bootstrapped FET follower

Figure 10.23 Bootstrapped FET amplifier transient response, 1 μ s

10.3.4 Low-Z amplifier

Capacitive feedback can be used with a low impedance virtual-ground amplifier (Figure 10.24). This configuration has a feedback capacitance contributed by the coupling of the pickup plate to electrode C (Figure 10.25).

The capacitance between electrode C and the pickup plate produces the capacitive feedback, C_{cp} . Note that the effect of stray capacitance C_{stray} drops out if the gain of the amplifier is high.

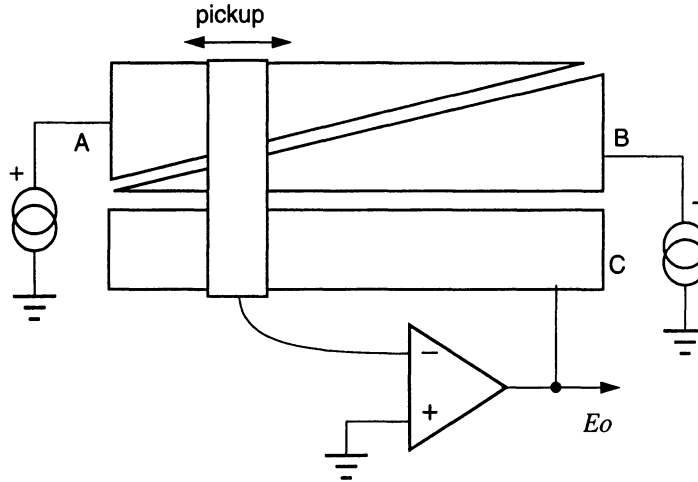


Figure 10.24 Low-Z amplifier with capacitive feedback

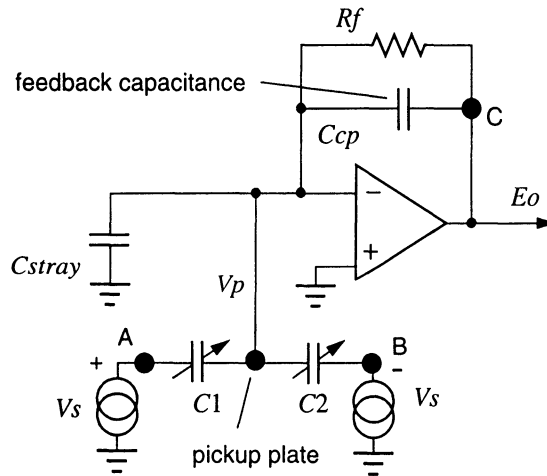


Figure 10.25 Equivalent circuit of low-Z amplifier

The amplifier output at frequencies well above the $R_f \times C1 \parallel C2$ time constant is

$$V_o = V_s \cdot \frac{C1 - C2}{C_{cp}} \quad 10.6$$

As C_{cp} and $C1 + C2$ are usually all on the same substrate and share a common spacing, the capacitance ratio and therefore the gain do not change with plate spacing. This circuit is a very useful way to build spacing-independent sensors. Also, amplifier input capacitance is not as important with a low-Z amplifier (but output-to-input capacitance is); the high-Z amplifier circuits must use low-capacitance operational amplifiers.

Although the example above was shown with ramp-shaped plates, any of the more tilt-resistant geometries work, and multiple-plate arrays also will work with this configuration.

10.3.5 Feedback amplifier

The guarded high-Z amplifier circuit (Figure 10.9) can be modified by referring the ground to the amplifier input and floating the stator drive circuits (Figure 10.26).

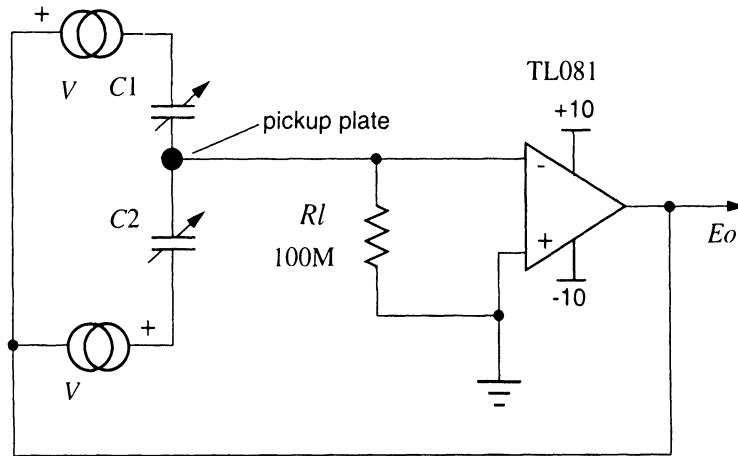


Figure 10.26 Feedback amplifier

With this circuit, the pickup plate is at virtual ground, so stray capacitance from pickup plate to ground is unimportant. This plate and its connection to the amplifier still need to be shielded with ground, however, as electrostatic pickup of noise sources is still a problem. The output voltage if $X_c \ll R_f$ is

$$\frac{E_o}{V} = \frac{C_1 - C_2}{C_1 + C_2} \quad 10.7$$

This circuit performs well but suffers from the need to float the exciting voltage. A coupling transformer or a two-op-amp circuit or summing circuits as shown in Figure 4.8 can replace the floating drives.

T configuration

A high-value resistor R_f may be used across C_{cp} in Figure 10.25 to set the DC level at the amplifier output. The time constant $R_f \times C_{cp}$ should be much larger than the period of the clock to avoid tilt in the output waveform. For a 20 kHz system, a time constant of 250 μ s can be used; then if C_{cp} is 1 pF, R_f should be 250 M Ω . Very large value resistors can be avoided (at the cost of greater output DC offset) by using smaller value resistors in a T configuration.

The T configuration (Figure 10.27) schematic shows the use of smaller value 1M resistors to simulate a 500 M Ω amplifier input resistance. This circuit has also a 500 \times

increase in DC offset voltage. If the increase in offset is a problem, a bypass capacitor C_b is added in series with the $2\text{ k}\Omega$ resistor, with a value which produces an acceptable $C_b \times 2\text{ k}\Omega$ time constant.

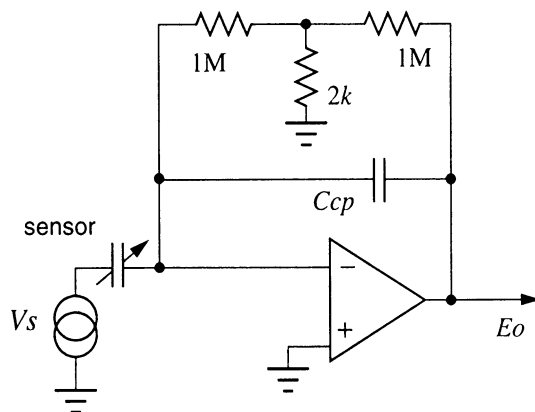


Figure 10.27 T configuration

10.3.6 Wireless connection

With one additional plate, Figure 10.24 can be made without wires. This works better with the low-Z connection of the op amp than with the high-Z connection (Figure 10.28).

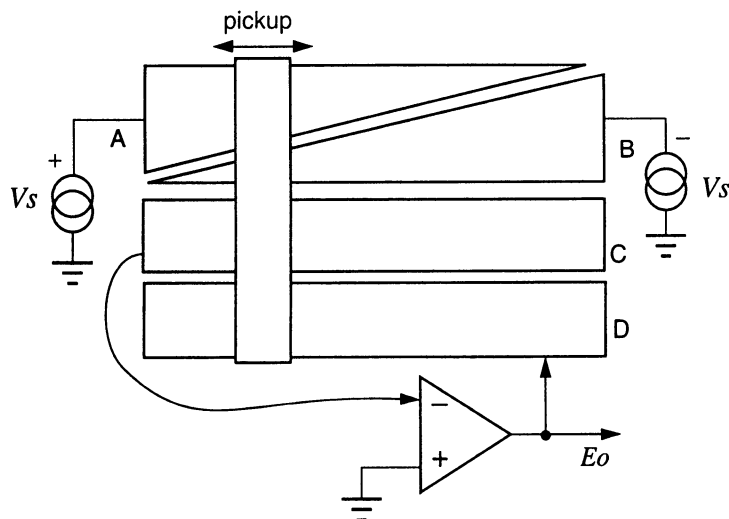


Figure 10.28 Low-Z, capacitive feedback without wires

Plate D has been added to Figure 10.28 to couple the amplifier's output back to the pickup plate without wires. For lower stray capacitance, a grounded plate should separate plates B and C and also C and D . The equivalent circuit is shown in Figure 10.29.

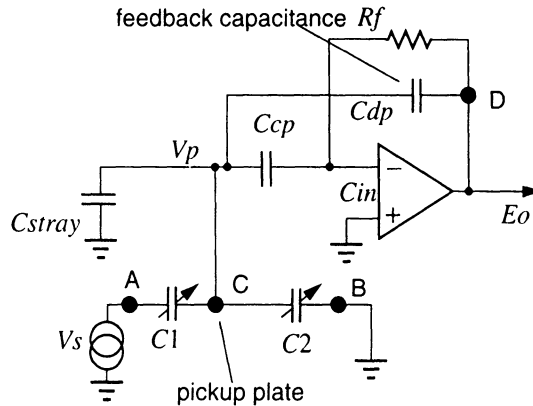


Figure 10.29 Wireless equivalent circuit

As in the previous circuit, a large value resistor R_f is included to set the DC output. The time constant $R_f \times C_{dp}$ should be several times larger than the period of the signal, or the T connection can be used to multiply R_f 's value.

The amplifier gain is reduced by the attenuation of the input coupling capacitor C_{cp} looking into the amplifier differential mode input capacitance C_{in} , or about 2–10 \times . Including allowance for this effect, the amplifier f_T should be 20–100 times the oscillator frequency.

FET input amplifier

With low-Z amplifier circuits like Figure 10.28, different stray capacitances become important compared to high-Z amplifiers. Capacitance from amplifier input to output now reduces signal, but input capacitance and other strays are not important. 1 pF of input-to-output capacitance will reduce amplitude by 50% if the pickup capacitance is 1 pF. This stray capacitance is not specified for IC op amps and is usually small, except in a dual op amp pinout where these pins are adjacent. In-out stray capacitance can be further reduced by adding an input preamp stage with discrete field-effect transistors (FETs) (Figure 10.30).

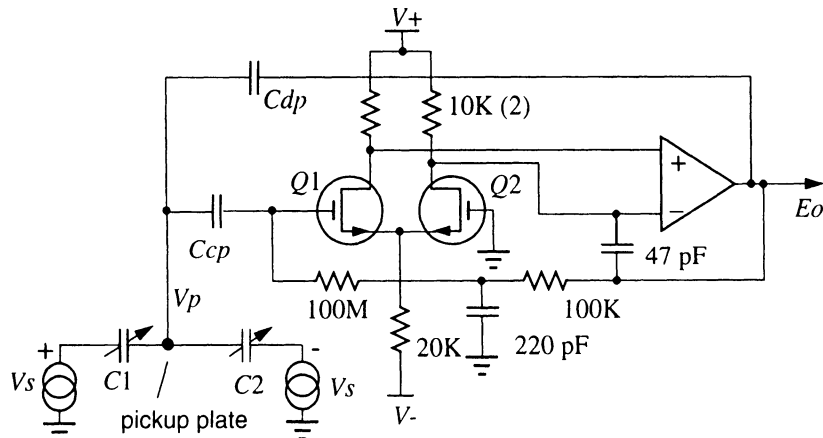


Figure 10.30 FET-input amplifier

The discrete FETs almost completely decouple the amplifier output from the input, and also improve AC parameters like noise, slew rate, and f_T , as the compromises of monolithic amplifier fabrication do not permit optimizing the input FET characteristics. This circuit can be constructed to have an infinitesimal value of input to output coupling, and because of this virtue it is suggested for use with extremely low values of sensor capacitance.

The 47 pF capacitor stabilizes the amplifier by reducing its 0-dB-gain frequency to compensate for the extra gain of $Q1$; in some cases a small (470 Ω –2 k Ω) resistor may also be needed in series with the source of $Q1$ to reduce the gain of this stage. $Q2$ can be deleted and the amplifier's negative input connected directly to a DC reference, say 2.5 V, if DC offset is not a problem. An advantage of this circuit is that a bipolar input op amp can be used, as the increased input current and current noise of bipolar amplifiers compared to FET versions are not important here.

10.4 NOISE PERFORMANCE

Current noise

With small values of pickup capacitance, low amplifier input noise current is needed. If, for example, a 1 pF pickup capacitance is used, with this sensor capacitance its impedance at a typical signal frequency of 25 kHz will be 6.4 M Ω . If the bipolar MC33077 were used, from Table 10.2, its current noise is 0.6 pA/ $\sqrt{\text{Hz}}$. Notice that 0.6 pA is the noise measured in 1 Hz bandwidth; the noise increases as the square root of bandwidth. This current noise produces 18 pA of noise in a bandwidth of 1 kHz, for an unsatisfactory input-referred noise voltage of 120 μV rms.

Crossover resistance

The other amplifiers listed in the table are FET input types and will have lower current noise contribution, a significant advantage with pickup capacitance less than a few pF. The amplifier crossover resistance R_c is the equivalent source resistance at which the typical current noise i_n of the op amp becomes larger than the voltage noise e_n . Larger values of crossover resistance are better. For the National LMC6081A1, for example, with a circuit resistance (as viewed from the op amp input terminal) of 90 M Ω , the amplifier current noise and voltage noise contribute equally to the total output noise. The amplifier-noise figure of merit for a sensor with an impedance X_c is $e_n + R_c/X_c$. Smaller values are better.

For input impedances less than R_c , voltage noise predominates. An amplifier with an R_c greater than the impedance of the electrode system is desirable, although the amplifier voltage noise is also significant. As the voltage noise of most amplifiers falls in a fairly narrow range between 4 and 40 nV/ $\sqrt{\text{Hz}}$, the noise at the amplifier output is usually minimized if R_c is larger than the circuit impedance.

Noise resistance

Another noise resistance R_n can be defined as

$$R_n = R_v + \frac{X_c^2}{R_i} \quad 10.8$$

where R_v is a resistor value which generates a thermal noise of the same magnitude as the amplifier input voltage noise, R_i is a resistor value which generates a thermal current equal to the amplifier input current, and X_c is the impedance of the sensor capacitance. Smaller values of R_n are better. For FET transistors, R_n is on the order of 1 k Ω , improving for larger geometry devices.

Resistor thermal noise

The thermal noise in a resistor R (see also Section 12.1.1) is

$$E_t = \sqrt{4kTRB} \quad 10.9$$

where

$$4kT = 1.64 \times 10^{-20} \text{ W-s at } 25^\circ\text{C}$$

B = noise bandwidth, Hz

For a 1M resistor and 1 kHz noise bandwidth at 25°C, $E_t = 4.06 \mu\text{V}$.

10.4.1 Circuit noise

Feedback circuit

The noise performance of the feedback circuit with a sensor capacitance of C_t and an exciting voltage of V_s can be calculated based on this equivalent circuit (Figure 10.31):

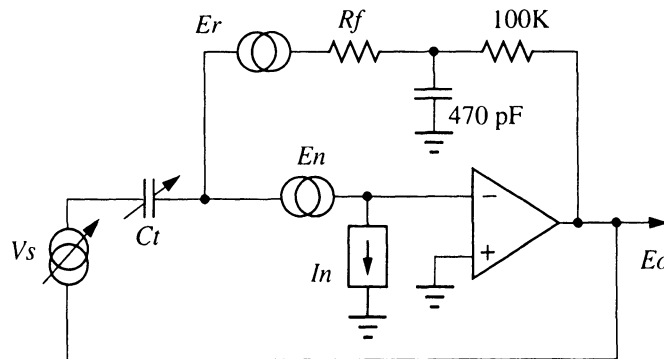


Figure 10.31 Noise model, feedback circuit

- R_f sets the DC output to zero
- E_n , I_n are the amplifier's equivalent input voltage and current noise generators
- E_r is R_f 's thermal noise
- The 100 k Ω / 470 pF lowpass filter (3 kHz) is included so that the input impedance is not reduced by R_f

With high op amp gain and high op amp input impedance, and assuming R_f is large, the output noise E_{no} is

$$E_{no}^2 = (E_o - V_s)^2 \cong E_n^2 + \left(\frac{I_n}{sC_t}\right)^2 + \left(\frac{E_r/R_f}{sC_t}\right)^2 \quad 10.10$$

Output noise decreases with increasing operating frequency and increasing sensor capacitance, and output noise decreases with increasing R_f until $R_f = R_c$. This behavior is also true for the other amplifier configurations, and eq. 10.10 is similar for noninverting amplifiers with a gain of 1 or inverting amplifiers with a gain of 1. For the best noise performance with a given sensor capacitance C_t :

- Choose an amplifier with high R_c , greater than $1/\omega C_t$, and low E_n
- Maximize the excitation voltage V_s
- Increase R_f so it is greater than R_c , or replace it with a noiseless switch circuit to sample output DC back to the input
- Increase the excitation frequency so that the impedance of C_t is less than R_c

Under these conditions the output noise will be close to E_n , and the signal-to-noise ratio E_{no}/E_n will be V_s/E_n . Although sensor series resistance is not included, its effect is minimum. If this resistance is 10 k Ω , for instance, it will cause a noise voltage of 12 nV/ $\sqrt{\text{Hz}}$, about the same as an op amp. Also, the stray capacitance to ground at the sensor should be less than the sensor capacitance. If $C_{stray} = C_t$, the noise will increase by 1.414.

Evaluating the output noise for the Texas Instruments CMOS-input operational amplifier TLE2061 with the following operating conditions:

$$\text{freq} = 20 \text{ kHz}$$

$$R_f > R_c = 100 \text{ M}\Omega$$

$$E_r = 4 \text{ }\mu\text{V}$$

$$C_t = 1 \text{ pF}$$

$$Z_{C_t} = 1/\omega C = 8 \text{ M}\Omega$$

$$\Delta f = 100 \text{ Hz (noise measurement bandwidth)}$$

the output noise voltage is

$$E_{no} \cong 0.11 \cdot 10^{-6} \text{ V rms}$$

The additive noise is considerably less than 1 μV , even with the small sensor capacitance.

10.5 COMPONENTS

10.5.1 Operational amplifiers

Operational amplifiers suitable for capacitive preamps have a high input impedance, high slew rate, high f_T , low power supply current consumption, and low current noise. The optimum input resistance for minimum noise, R_c , equal to the noise voltage divided by the noise current, is also listed. Some examples are shown in Table 10.2.

Table 10.2 Low-current-noise operational amplifiers

Mfgr.	Type	f_T MHz typ	Slew rate V/ μ s typ	I_{bias} 25°C typ	I_{supply} mA per amp typ	Voltage noise nV/ $\sqrt{\text{Hz}}$ 1 kHz	Current noise fA/ $\sqrt{\text{Hz}}$ 1 kHz	Cross resist. R_c	Notes (JFET types except where noted)
Analog Devices	AD549	1	3	100 fA	0.6	35	0.11	318 M	$Z_{in}=10^{13} \Omega$, 1 pF
Analog Devices	AD820/822	1.8	3	10 pA	0.6	16	0.8	20M	Single supply, rail-to-rail output, input CMR includes gnd
Analog Devices	AD823	16	20	3 pA	2.6	16	1	16M	Dual, 3 V, rail-to-rail
Burr-Brown	OPA129	1	2.5	± 30 fA	1.2	27	0.1	270 M	$Z_{in}=10^{13} \Omega$, 1 pF
Harris	CA5160	15	10	2 pA	2	30 ^a	N/A	--	MOSFET ^b
Linear Tech	LT1169A	5.3	4.2	1 pA	5.3	6	0.8	7.5 M	Dual
Motorola	MC35081	8.0	25	60 pA	2.5	38	10	3.8 M	$C_{in} = 5$ p
Motorola	MC33077	37	11	280 nA	1.75	25	600	42 k	Dual, bipolar
National	LMC6081	1.3	1.2	4 pA	0.85	--	0.2	90 M	CMOS ^c
National	LM6142	17	30	280 nA	0.88	16	220	72 k	1.8–24 V supply, rail-to-rail input and output, bipolar
National	LMC6482	1.5	0.6	0.02 pA	0.9	37	30	1.2 M	Dual; 3–15 V supply, rail-to-rail input and output
T.I.	TLE2061	1.8	3.4	3 pA	0.28	43	1	60 M	--
T.I.	TLE2082	10	35	15 pA	1.5	16	2.8	15 M	Dual
T.I.	TLC271	17	3.6	0.6 pA	0.9	25	--	--	@high bias; 3–16 V supply
T.I.	TL081	4.0	13	--	1.8	--	10	3 M	--

^aAt 10 kHz^b16 V max supply^c16 V max supply; common mode input range includes ground

The devices with bias current higher than 1 nA are bipolar-input types which are not directly useful for this application because of high current noise, but can be used if preceded with a discrete FET preamplifier. Other amplifiers, unless noted, are FET input

types with one amplifier per package. The FET input amplifiers show much smaller bias currents and much lower current noise than the bipolar types. The supply current can be important in the follower connection where the negative supply is bootstrapped.

10.5.2 Resistors

High-value resistors

Most resistors are conveniently available in values ranging from 10 Ω to 10 M Ω . 100 M Ω resistors and over are a specialty item available from several suppliers, including Ohmtek, 2160 Liberty Drive, Niagara Falls, NY 14301, (716)283-4025 and Ohmcraft, Inc., 3800 Monroe Ave., Pittsford, NY 14534, (716)586-0823. These companies are subsidiaries of Vishay Resistive Systems of Malvern, PA. Ohmcraft's fine line thick film technology produces resistors with these specifications (Table 10.3).

Table 10.3 High value resistor specifications

Resistance	10M	100M	1000M	10,000M
Tightest tolerance	1%	5%	5%	10%
TCR, 25–75°C, ppm/°C	25	50	100	150
Voltage rating	500 V	500 V	1000 V	1000 V
VCR, ppm/V	<10	<10	<10	<10

Chip resistors are available in 0502 (5 × 2.5 mm) size with less than or equal to 100 G Ω resistance, and larger sizes such as the 2512 (25 mm × 12.5 mm) can have 3.5 T Ω resistance, a DC voltage rating of up to 2500 V, and 2 W power ratings.

10.6 CARRIER

Frequency of operation

As the operating frequency is increased, the impedance of the capacitive sensor drops. This is usually valuable, as for small sensor dimensions the capacitance may be a fraction of a pF. With 0.01 pF capacitance at 10 kHz

$$X_c = \frac{1}{2\pi fC} = 159 \text{ M}\Omega$$

At this impedance it will be difficult to obtain a good signal to noise ratio, with additive amplifier current noise and capacitive crosstalk being the main noise sources. With the frequency increased to 200 kHz, an amplifier with a sensor capacitance of 0.01 pF will have an output noise approaching the noise voltage of the amplifier and a signal-to-noise ratio with a 5 V excitation of about 170 dB.

But high frequency operation has two problems, power and ease of demodulation. Power increases because higher frequency amplifiers are needed, and demodulation is

more difficult as sine wave signals must be used rather than square wave to avoid risetime induced nonlinearities. With a lower frequency carrier, say 40 kHz square wave, the amplifier bandwidth should be roughly 400 kHz to preserve good waveform shape, and CMOS switches can be conveniently used for demodulation. With a 1 MHz carrier, good square wave fidelity would mandate a 10 MHz amplifier and < 50 ns switches. These parts would have considerable power consumption.

Sine wave carrier

Sine wave sensor excitation can be used, but amplifier bandwidth should still be a large factor higher than the carrier frequency for good closed-loop gain stability, and sine wave demodulation will require high frequency multipliers and other expensive parts. In general, simpler circuits can be built in the 10 – 100 kHz range using operational amplifiers with 1 – 10 MHz bandwidth and CMOS switches of the 74HC4053 type which switch in the 100 ns range. For critical circuits, the sine wave carrier offers some benefits to offset the extra cost:

- A narrow bandwidth tuned circuit can precede the amplifier to attenuate out-of-band noise
- Small timing variations between the sensor excitation signal and the demodulator reference signal do not contribute to drift
- Spikes and noise are reduced
- A lower frequency amplifier can be used, and the amplifier slew rate is usually unimportant

Also, a sine wave drive is essential for capacitive micrometers or other circuits where the amplifier gain is increased in order to expand the range. For example, if plate deflection in a balanced bridge were only 1% of the total distance, the amplifier gain would be increased by 100 \times to produce a full scale output. In this case, the bridge is adjusted for null by tweaking an adjustable leg to balance the output to zero with no deflection. With square wave drive, the bridge must successfully balance not only the fundamental, but all of the square wave harmonics, or the amplifier at null will output excess harmonic energy. When the fundamental is completely nulled, it is likely that nonlinear effects will cause the higher harmonics to feed through, spoiling the null and possibly saturating the amplifier output. A tuned input circuit with passive components can remedy the problem, or sine wave drive may be more convenient.

Sine wave generation

Sine wave sensor excitation has advantages of avoiding slew rate limit and nonlinear phase shift problems. At high frequencies, sine waves produce less EMI and are preferred for applications which radiate energy such as proximity detectors. For sensitive applications, sine wave excitation or a bandpass immediately preceding the amplifier are suggested. Sine waves do not need to have particularly good distortion characteristics for sensor use; more important is amplitude stability; this tends to rule out traditional sine wave oscillator circuits such as Colpitts and Wein Bridge oscillators. Several techniques

can be used to produce sine waves with timing derived from a quartz crystal oscillator and with very stable amplitude:

1. Square wave with lowpass filter
2. DAC with sine coefficients
3. Finite impulse response (FIR) digital filter

The square wave with lowpass filter is easiest to build, but it adds a phase shift which may not be stable. If the same square wave signal is used to synchronize the demodulator, the phase shift produced by the filter must be equalized in both paths for accurate demodulation. One method is to use a comparator to square up the filter-output sine wave for the demodulator.

Methods 2 and 3 can use a coarse 3 bit DAC or a very short three-tap FIR lowpass filter to produce sine waves with no 2nd through 4th harmonic distortion. Higher order harmonics may be ignored, or can be easily attenuated with a low-phase-shift one-pole lowpass filter.

Square wave generation

Square wave generation is simple with CMOS logic, as this logic pulls the high impedance of the typical capacitive sensor to the power rails very accurately. With a low-value resistive load, say less than 10 k Ω , a low impedance family such as the 74AC series can be used. See also Section 10.6.

10.7 DEMODULATORS

10.7.1 180° drive circuits

Two different types of square wave drive voltages are useful, 90° and 180°. The 180° driver is the simplest and is used for sensors which have a stable electrode spacing, or for systems with moderate total accuracy requirements (Figure 10.32).

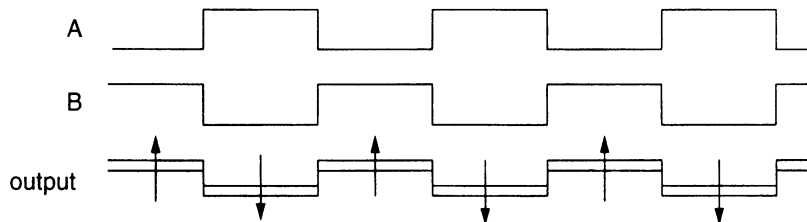


Figure 10.32 180° drive waveforms

These drive signals can be conveniently and accurately generated by CMOS logic gates, such as the 74HC04. With 5 V logic, as the pickup plate moves from A to B, the output varies from 0° (5 V p-p), through zero, to 180°. A ratiometric area-variation motion sensor with a 180° drive is shown in Figure 10.33.

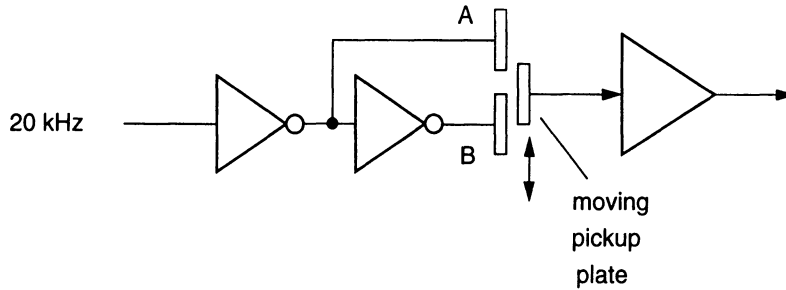


Figure 10.33 180° drive circuit

For simple circuits, only one plate needs to be driven, with the other plate at ground. Driving both plates gives $2\times$ signal swing and produces a ground-centered output.

A commercial demodulator for 180° drives is available from Analog Devices, the AD698 (Figure 10.34). It is intended to be used as a demodulator for linear variable differential transformer (LVDT) sensors, but it is also used as a capacitive sensor demodulator.

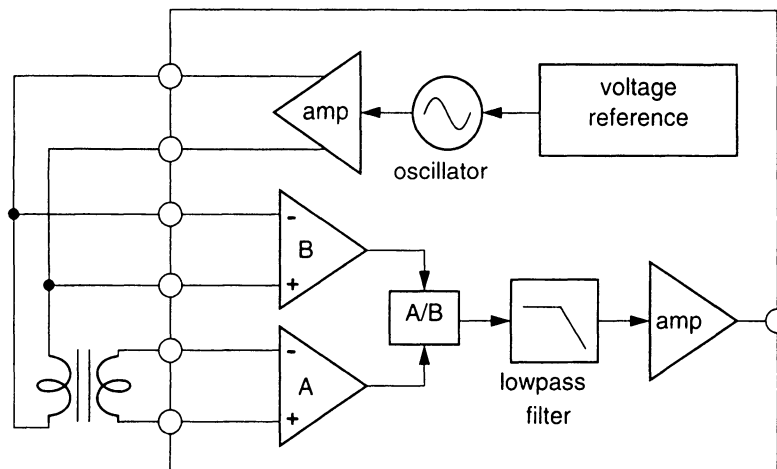


Figure 10.34 AD698 demodulator

The stabilized oscillator produces a low distortion 20 kHz sine wave drive with up to 24 V p-p rms with a ± 15 V supply. The B channel input is a synchronous demodulator which detects the excitation voltage amplitude, and the A channel input is a second synchronous demodulator. The use of the B channel as a reference means that the oscillator amplitude stability is unimportant. A divider produces an accurate ratiometric output which is lowpass filtered and buffered, and the divider output is the ratio of the transformer output to the excitation voltage amplitude. The typical gain error is 0.1%, and typical nonlinearity is 75 ppm of full scale. The input impedance is 200 k Ω , as the device was designed for low-impedance inductive sensors, so a buffer must be used for most capacitive sensors (Figure 10.35). If reference capacitors with the same construction as the sense

capacitors and a second amplifier are added to the B input, temperature effects and amplitude variations caused by spacing change may be compensated.

A similar device without the ratiometric feature and with less accuracy, Analog Device's AD598, may also be used, or the AD2S93 may be used if its internal 14 bit ADC is needed.

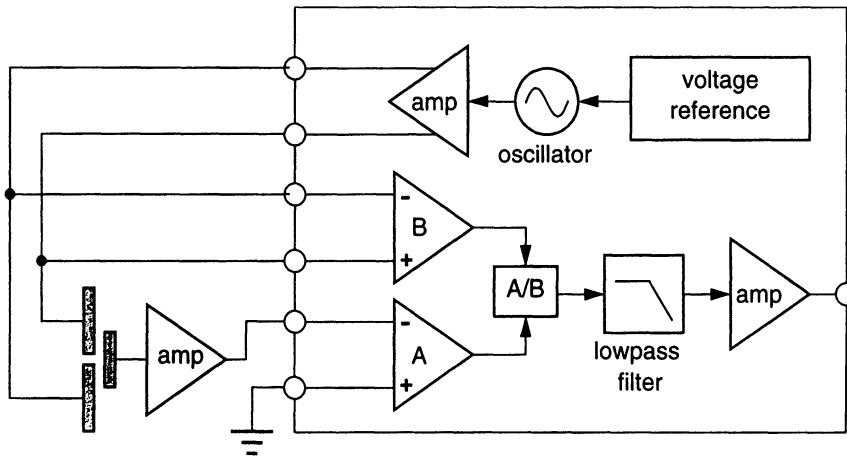


Figure 10.35 AD698 with bridge-type capacitive sensor

10.7.2 90° drive circuits

For improved performance with variable spacing, 0 and 90° excitation signals are needed (Figure 10.36).

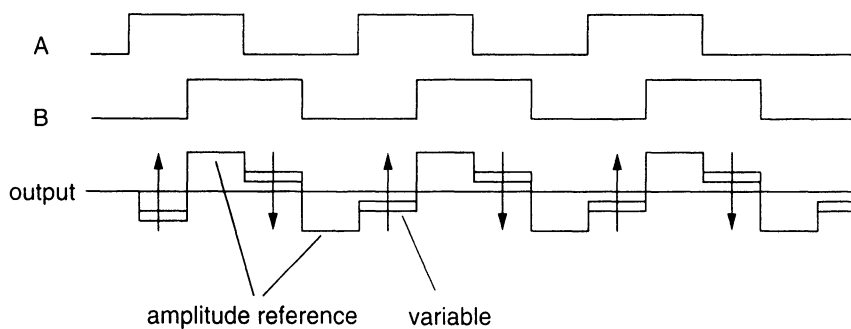


Figure 10.36 90° drive

With the 90° drive, the output has an amplitude reference, alternately reversing polarity, which does not change amplitude with pickup plate position. Between amplitude reference segments, the variable segments also alternately reverse polarity as shown, and change amplitude in response to motion. This allows amplitude-independent ratiometric demodulation which is useful for systems with poor mechanical gap tolerances or gap variation with position; during each cycle the ratio of the variable segment to the fixed

amplitude reference is measured. The demodulator can accommodate large amplitude changes without compromising output accuracy.

Amplitude reference

The reference segments can be used in two ways: as an AGC signal, to control the gain of a variable-gain amplifier, or as a reference for an analog-to-digital converter or a voltage-to-period converter. In either case, the circuit output is the ratio of a variable segment to an amplitude reference segment. The graphic input tablet described in Chapter 19 shows how this circuit may be implemented.